Research Article

Hongyuan Tang*, Xuezhi Deng, and Xiaojun Zhou

Experimental study on behavior of steel channel strengthened with CFRP

https://doi.org/10.1515/cls-2017-0019
Received May 18, 2017; accepted Jul 13, 2017

Abstract: This paper describes the behaviour of axially loaded long and eccentrically loaded short thin-walled steel channels, strengthened with transversely bonded carbon fibre reinforced polymer (CFRP) sheets. Seven long members, each 1400 mm long, and seven short members, each 750 mm long, were tested. The main parameters were the number of CFRP plies (one or two) and the clear spacing between the CFRP strips (50, 100 or 150 mm). The effect of CFRP sheet layer and clear spacing was studied. All the ultimate load capacity of the reinforced members was improved in different extent. A maximum strength gain of 9.13% was achieved for long members with two CFRP layers and 50 mm spacing of CFRP strips. The experimental results show that the global buckling happens to all the long specimens. For short members, the maximum strength gain of 12.1% was achieved with two CFRP layers and 50 mm spacing of CFRP strips. With the exception of the most heavily reinforced (2 plies at 50 and 100 mm), local buckling was observed prior to global buckling for short members, which was completely opposite of the control specimens. Meanwhile, when the clear spacing of CFRP strips is greater than the web height of steel channel, the transversely bonded CFRP does not have a significant improvement in buckling load capacity of the short- and long-channel components. While the clear spacing is less than the web height, the more number of CFRP layer, the more enhancement of buckling load capacity.

Keywords: Retrofit, steel, thin-walled, channel, CFRP, buckling

1 Introduction

The use of fibre-reinforced polymer (FRP) sheets has been successfully demonstrated in retrofits of concrete structures. However, research on using FRP in the retrofit of steel structures has been fairly limited [2, 7, 23]. Most of the research conducted in this area has focused on three parts: firstly, retrofit the beam with CFRP, including reinforcing damaged steel beams [3, 9, 10, 12, 16] and undamaged steel beams [4, 5, 14]. These works show that the ultimate load capacity of steel beams was improved after reinforced with CFRP; secondly, using CFRP to reinforce the axial compressive steel members [6, 8, 11, 13, 15, 19, 21], the reinforced specimen section includes the T, H, circular and square tube section. These literatures indicate that the CFRP can improve the flange and web local buckling or flexural torsional buckling load capacity. Finally, using CFRP to retrofit the fatigue resistance of steel structures [20, 22], the remaining fatigue life was multiply improved after reinforcement.

All the previous work shows that the proper CFRP constraints can increase the buckling load capacity or the remaining fatigue life of members to different degrees. No research, however, has been reported on the strengthening of thin-walled steel channel under axial compression, particularly research to examine the effect of CFRP sheets on the local and global buckling behaviour of long or short steel channels. Given that the cold-formed thin-walled channel specimen is uniaxial symmetry, it is very easy to occur the flange buckling, web local buckling and flexural torsion. This paper, therefore, is focused on evaluating the effectiveness of CFRP-reinforced long and short thin-walled steel channels subject to axial and eccentric load; meanwhile, buckling behaviors and the associated failure modes were described. In addition, the influence of CFRP layer and clear spacing of transverse CFRP strips was investigated.

***Corresponding Author: Hongyuan Tang:** College of Architecture and Civil Engineering, Xihua University, Chengdu 610039, China; Email: tanghyseu@163.com
Xuezhi Deng, Xiaojun Zhou: College of Architecture and Civil Engineering, Xihua University, Chengdu 610039, China

2 Experimental Program

2.1 Material Properties

According to the specification [17], the test specimens were made of Q235 steel whose tangent modulus of elasticity, yield and ultimate strength were 202 GPa, 305.8 MPa and 418.5 MPa. Poisson ratio was 0.3, and the ultimate elongation was 0.33. The material performance of CFRP is shown in Table 1, and the mixture ratio of the adhesive to the curing agent was 3:1. Using manufacturer-prescribed saturant, the elastic modulus, tension, compression and shear strength of the adhesive were 380 GPa, 43.5 MPa, 86.0 MPa, 22.06MPa, and the ultimate elongation was 0.022.

Table 1: Material properties of CFRP

Model	t_f mm	f_{td} MPa	E_f GPa	ϵ_u -
CJT-300I	0.167	3400	240	0.017

2.2 Fabrication of Test Specimens

An experimental program has been carried out to investigate the feasibility of using CFRP sheets for retrofitting of steel channels of two different slenderness ratios, selected to simulate short- and long-channel conditions. A total of 7 short and 7 long specimens, as shown in Table 2, were tested. Some of the tests were conducted on control specimens, without any CFRP retrofitting system; the rest of the tests were conducted on CFRP retrofitted specimens. The number of CFRP layers and clear spacing were varied. The steel channel specimens were cut to the desired lengths. Care was taken to ensure flat ends. All specimens were cured for at least 6 days at room temperature, prior to testing, as recommended by the manufacturer.

Except two control specimens (SC0 and LC0), around the internal and external sides of the rest twelve specimens were all transversely bonded with 50 mm wide CFRP strips, as shown in Figure 1. Strips were one or two layers thick (n) and provide a clear spacing of s = 50, 100 or 150 mm, as shown in Table 2.

In order to facilitate the loading, two ends of the specimen were welded with a steel plate respectively. For the sake of extra constraint, only use spot-weld while welding the ends plate.

For flexure, sections are classified as compact, noncompact or slender-element sections. If the width-to-thickness ratio of compression elements exceeds λ_p, but does not exceed λ_r, the section is noncompact. The parameters λ_p and λ_r are described as equation (1) and (2) for the limiting ratio (b/t) respectively. And the parameters λ_p and λ_r are described as equation (3) and (4) for the limiting ratio (h/t_w) respectively [1].

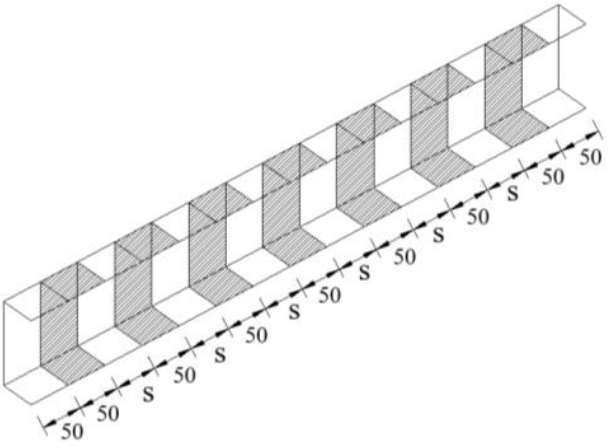

Figure 1: Test specimen

$$b/t: \quad \lambda_p = 0.38\sqrt{\frac{E}{F_y}} \tag{1}$$

$$b/t: \quad \lambda_r = 1.0\sqrt{\frac{E}{F_y}} \tag{2}$$

$$h/t_w: \quad \lambda_p = 3.76\sqrt{\frac{E}{F_y}} \tag{3}$$

$$h/t_w: \quad \lambda_r = 5.7\sqrt{\frac{E}{F_y}} \tag{4}$$

where, the limiting ratios (b/t), λ_p and λ_r, are equal to 9.77 and 25.7 for short channels under eccentrically load respectively. Obviously, these sections have noncompact flanges.

For compression, sections are classified as nonslender element or slender-element sections. If the width-to-thickness (b/t) ratio of compression elements exceeds λ_r, the section is a slender-element section. The parameters λ_r is determined as following equation (5) [1].

$$b/t: \quad \lambda_r = 0.56\sqrt{\frac{E}{F_y}} \tag{5}$$

$$h/t_w: \quad \lambda_r = 1.49\sqrt{\frac{E}{F_y}} \tag{6}$$

where, the limiting ratio (b/t), λ_r, is equal to14.39 for long channels under axial load. So, their sections have slender flanges.

Table 2: Parameters of specimens

Specimen label	L mm	Size (Actual Value) mm	kL/r -	b/t -	h/t_w -	Number of Reinforcement Ply	s mm
SC0	750	100.5×42.5×2.62	62	16.2	36.4	0	0
SC1	750	100.0×42.8×2.63	61.5	16.3	36.0	1	50
SC2	750	101.4×42.1×2.61	63	16.1	36.9	2	50
SC3	750	100.9×41.8×2.64	63.6	15.8	36.2	1	100
SC4	750	100.6×42.6×2.63	62	16.2	36.3	2	100
SC5	750	100.9×41.9×2.62	63.6	16	36.5	1	150
SC6	750	100.6×42.4×2.61	62.5	16.2	36.5	2	150
LC0	1400	102.5×43.5×2.62	112.9	16.6	37.1	0	0
LC1	1400	102.1×42.8×2.63	112.9	16.3	36.8	1	50
LC2	1400	101.4×43.1×2.61	113.8	16.5	36.9	2	50
LC3	1400	101.9×43.8×2.64	112	16.6	36.6	1	100
LC4	1400	101.6×43.6×2.63	112.9	16.6	36.6	2	100
LC5	1400	101.9×43.1×2.62	113.8	16.5	36.9	1	150
LC6	1400	101.6×43.0×2.61	114.8	16.5	36.9	2	150

2.3 Test setup and instrumentation

In order to collect the deformation and strain of the specimens, the LVDT (linear variable differential transducers) and the strain gauges were respectively arranged on the specimens, and the positions were shown in Figure 2. At the midheight of a specimen, three longitudinal orientations of the strain gauge were arranged at the middle of the web and two flanges. The vertical deformation of a specimen was measured by a hydraulic servo loading control system and LVDT ⑤. The transverse deformation was measured by LVDT ①. LVDTs ①, ②, ③, and ④ were respectively arranged at the midheight of the web and flanges of a specimen, while LVDTs ⑥ and ⑦ were located above and below LVDT ② at 150 mm. In addition, two cameras were set on both sides of the loading device to record the entire test process.

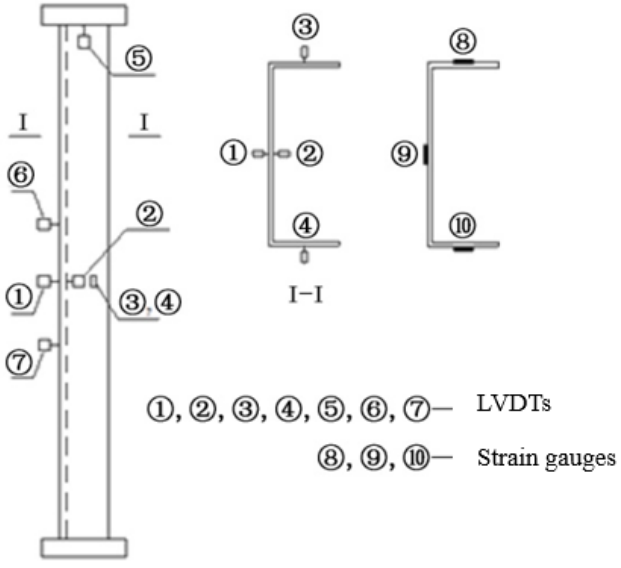

Figure 2: The arrangement of LVDTs and strain gauges

The test used 500 kN hydraulic servo loading system, and the details of the component were shown in Figure 3. In order to ensure that the tested specimen was hinged at both ends, two ends were respectively provided with two hinged supports. And two hinged supports were located at the center of the cross section of the channel.

The effective length factor (k) is assumed to be equal to 1.0 in this case, as the channels were hinged at both ends. Because of the low kL/r ratio for the short channels, it was anticipated that local buckling would govern failure after the steel reached the yield load. According to the code [23], for short thin-walled steel channel, the initial buckling capacity is about 74.2 kN. The preload is 3% of the estimation, loading slowly. Each load class has 2 to 3 minutes in order to collect the strain and deformation data. After the load is applied to 40 kN, each loading step changes to 1 kN per time. And then continue loading until the test component fails.

According to the code [18], the length of the long channels was chosen to be 1400 mm, to provide a slenderness ratio about weak-axis, which ensures the occurrence of overall buckling as long channels. Based on the code [23], for the long thin-walled steel channel, the stability capacity is about 57.5 kN. According to the estimation, the classification of the test load is as follows. The pre-loading is

(a) Top hinged support

(b) Bottom hinged support

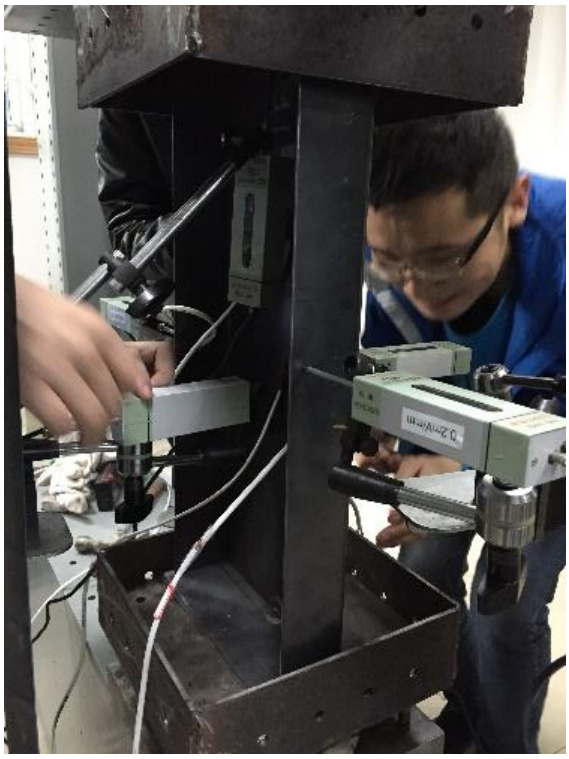

(c) Detailed of the LVDTs arrangement

Figure 3: Test setup

estimated by 5%, and the loading speed was slow. The formal loading phase requires 10% of the estimated load. Before testing, every effort to ensure a perfectly concentric loading condition.

3 Experimental Results

In the following sections, test results are presented in terms of the load–displacement and load–strain responses. The gains in both axial strength and eccentric strength of CFRP-retrofitted channels are presented. The effects of various parameters on the behaviour and failure modes are also discussed.

3.1 Failure modes of short and long specimens

Due to the relatively slender flange width-thickness ratio (b/t = 16.2) [21] and the load eccentricity, the typical failure mode for short-channel control specimen was yielding followed by symmetric local buckling, where two opposite flanges buckled outward, as shown in Figure 4. As the load was applied beyond the yield, specimens tended to twist, and the flange buckling did not occur at exactly the same height of the specimen. However, the six specimens reinforced with CFRP exhibited both flange local buckling (FLB) and flexural torsional buckling (FTB) as described in the following sections. As shown in Figure 4, the local flange buckling occurred above and below the midheight-located CFRP strip on each flange.

Figure 4: Failure modes of short specimens

Figure 5: Failure modes of long specimens

In all long-channel specimens, failure was mainly due to excessive overall bucking of the specimen (Figure 5), followed by a secondary local buckling failure in the compression flanges, near the mid-length of the specimen (Figure 5). Similar with the short-channel specimens, the local flange buckling occurred above and below the midheight-located CFRP strip on each flange.

In general, none of the short- and long-channel specimens failed at the CFRP joint overlap. And there was no delamination or rupture of CFRP during the whole test program.

A summary of test results, including yield load (P_y), ultimate load capacity (P_u), and buckling modes, is presented in Table 3. Also given in Table 3 is the percentage increases in capacity load for the CFRP-retrofitted specimens relative to the values for the control specimens.

Table 3: Summary of load capacity and buckling modes

Specimen	P_y	P_u	ΔP	Buckling
	kN	kN	%	modes
SC0	52	57.23	-	FLB
SC1	56	60.54	5.8	FLB
SC2	-	64.18	12.1	FTB
SC3	54	59.58	4.1	FLB
SC4	-	60.65	6.0	FTB
SC5	52	59.35	3.7	FLB
SC6	52	60.11	5.0	FLB
LC0	-	47.75	-	FTB
LC1	-	51.68	8.23	FTB
LC2	-	52.11	9.13	FTB
LC3	-	50.23	5.20	FTB
LC4	-	51.08	6.97	FTB
LC5	-	49.11	2.85	FTB
LC6	-	49.98	4.67	FTB

In Table 3, all the long-channel specimens exhibited flexural torsional buckling (FTB). As for the short-channel specimens, however, specimens SC2 and SC4 exhibited flexural torsional buckling (FTB) prior to their flanges buckling. This was attributed to the fact that these specimens a) had the greatest amount of CFRP applied (Table 1); and b) were reinforced at their midheight – the location of the greatest moment due to load eccentricity. Capacities of the CFRP-wrapped specimens (including long- and short-channel specimens, as shown in Table 3) were greater than that of non-retrofitted specimens.

3.2 Load-displacement curve of short specimens

The load – horizontal displacement curves for all short-column specimens are shown in Figure 6. In each graph, two curves are presented for the control specimen and the CFRP-retrofitted specimen.

The gain in axial strength for the CFRP-retrofitted specimens ranged from 3.17% to 12.1% (Table 3). Test results in Table 3 and Figure 6 indicate that for short-channel specimens, number of CFRP layers is more efficient in increasing the eccentrically load capacity than clear spacing of CFRP strips oriented in the transverse direction. The results also indicate that specimen SC2, with two transverse layers of CFRP and clear spacing of 50 mm, achieved the highest gain in strength, 12.1%.

3.3 Load-displacement curve of long specimens

The load versus lateral deflection of all long-channel specimens is shown in Figure 7. The gain in axial strength for the CFRP-retrofitted specimens ranged from 2.85% to 9.13% (Table 3). The strength gains, however, do not correlate directly with the number of CFRP layers. For example, specimen LC6 (two layers) shows only a 4.67% increase in strength, whereas LC1 (one layer) shows an 8.23% increase. This was attributed to the fact that specimens LC1 and LC6 had the different clear spacing of CFRP strips (Table 2).

The Figure 7 indicates that for specimens of comparable imperfections (control and LC2), the behaviour of the CFRP-strengthened specimen shows not only higher strength but also higher initial slope, compared to control specimen, which indicates that CFRP has improved stability against lateral deflections.

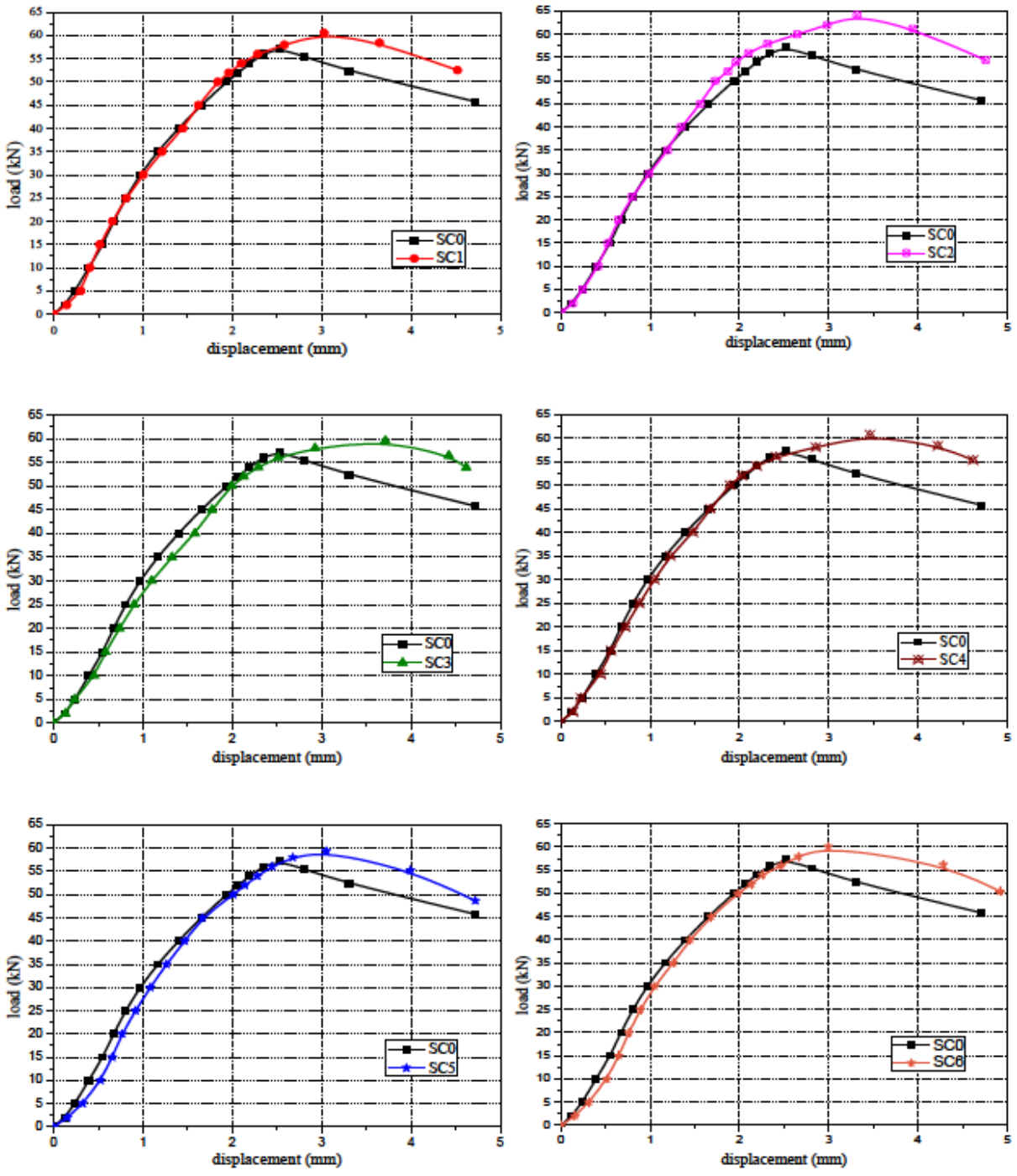

Figure 6: Load-displacement relationship of short-channel specimens under eccentrically load

3.4 Load-strain relationship of specimens

Figure 8 shows the load – axial strain behaviour of the control specimen and specimens retrofitted with transversely bonded CFRP. For the control specimen, gauge ⑩ showed linearly increasing compressive strains up to a certain point, where flanges local buckling took place. At this point, two flanges buckled outward, as indicated by the strains measured by ⑩, which reversed direction sharply as a result of the reduction of compressive strain. For the retrofitted specimens, strains measured by ⑩ indicate a more severe reversion at a certain point, which also occurred at a higher load level than with the control specimen. Furthermore, the difference between the gauge read-

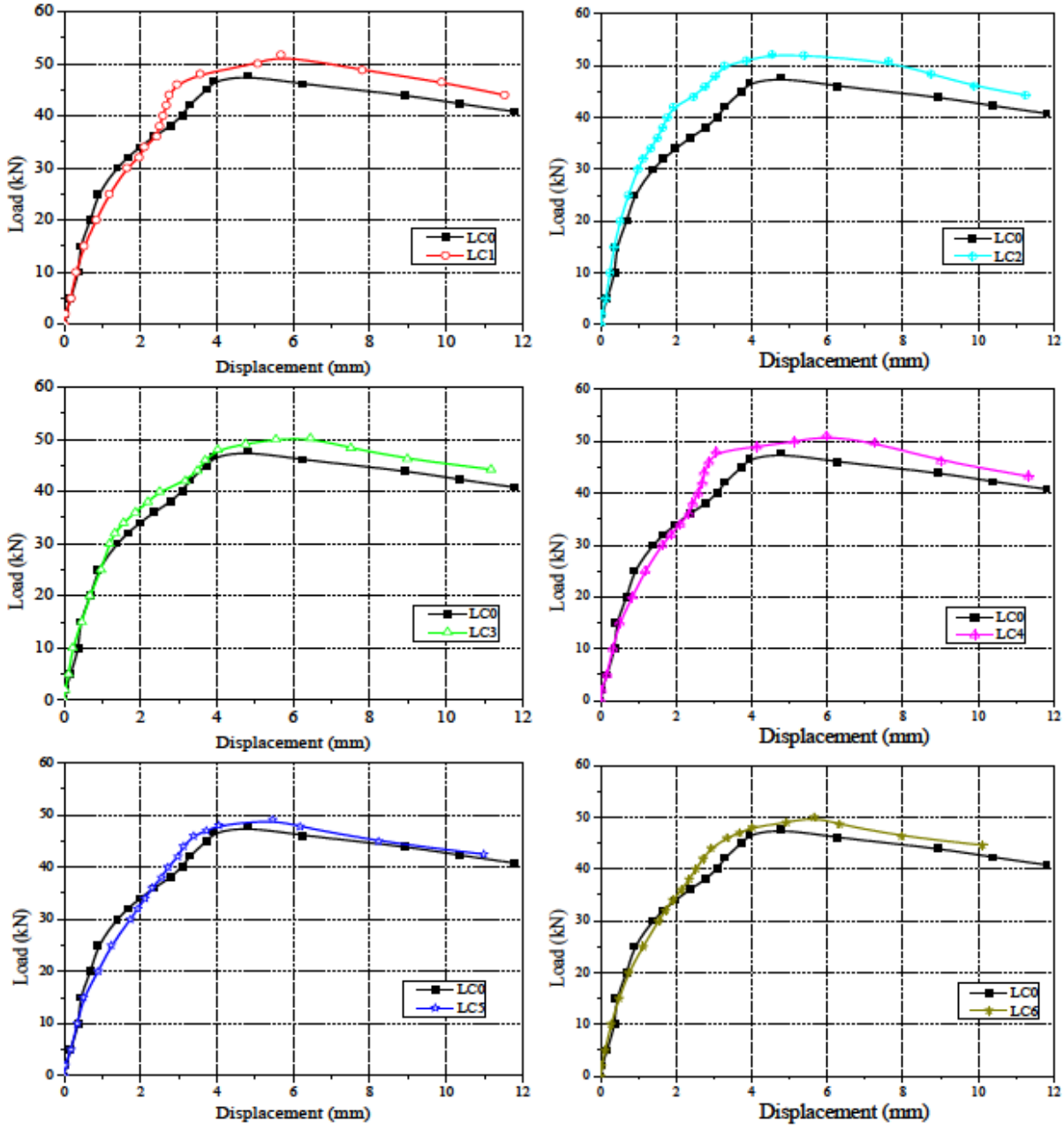

Figure 7: Load-displacement relationship of long-channel specimens under axial load

ings of the control specimen and retrofitted specimens at an early stage within the elastic range appears to be increased for specimens with CFRP, compared with the control specimen, which suggests that CFRP improves the stability of the specimens.

Figure 9 shows the load versus axial strain at the web side of all specimens, as measured by the strain gauge at the midheight. The figure shows that the web side is under compression up to a certain load, at which point excessive buckling occurs, and then, the strains in web side in compression change to tension. The strains indicate that global buckling starts at strain values far below the yielding strain of 0.0015, which suggests the existence of imperfections of different magnitude, possibly as a result of slight out-of-straightness in the specimens, minor misalignment within the test setup, or a combination of both.

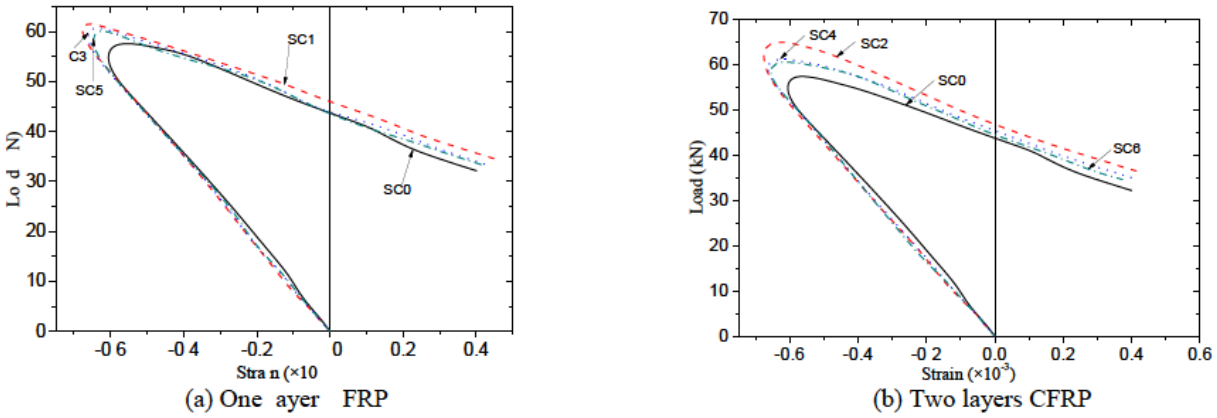

(a) One ayer FRP (b) Two layers CFRP

Figure 8: Load-strain relationship of short-channel specimens

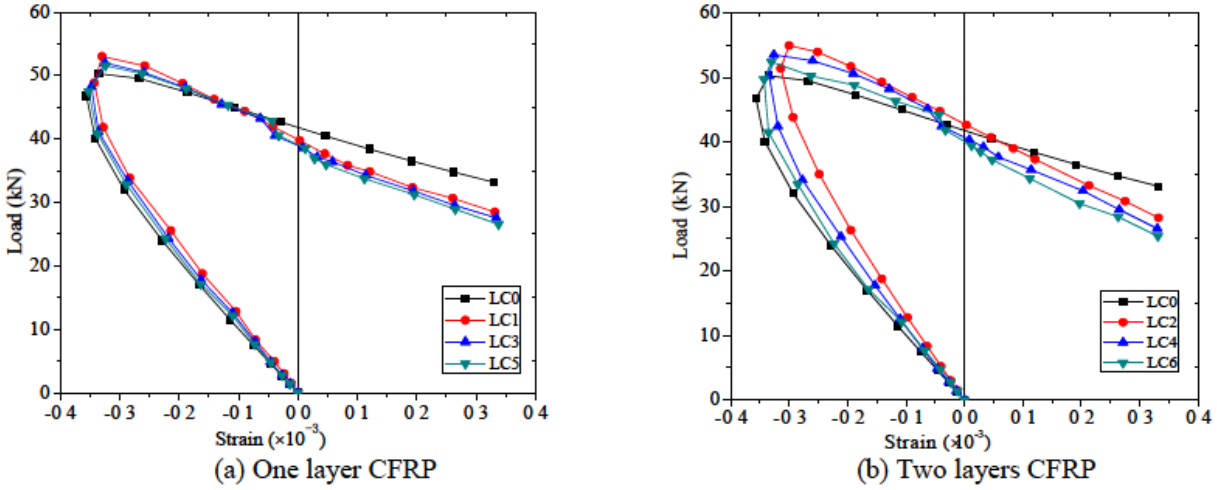

(a) One layer CFRP (b) Two layers CFRP

Figure 9: Load-strain relationship of long-channel specimens

4 Result and Discussion

4.1 Effect of CFRP on failure modes of specimens

Figure 10 shows a schematic of typical failure mode for short- and long-channel specimens retrofitted with transvers CFRP strips. The local flange buckling occurred just above and below the midheight-located CFRP strip on each flange. It seems to avoid the exact place where CFRP strips exist. From test, it was observed that two flanges would typically buckle outward.

In this study, for thin-walled sections, this type of deformation occurs before the cross-sectional yield load is reached. In Figure 10, it can also be observed that CFRP sheets could confine outward buckling and that transverse CFRP layers are effective in confining outward local buckling of the two opposite steel flanges. This confinement controls local buckling of steel channels, and it can improve the capacity of steel channels. Therefore, CFRP strengthening can delay local buckling by confining effect on outward local buckling sides, the maximum load can increase.

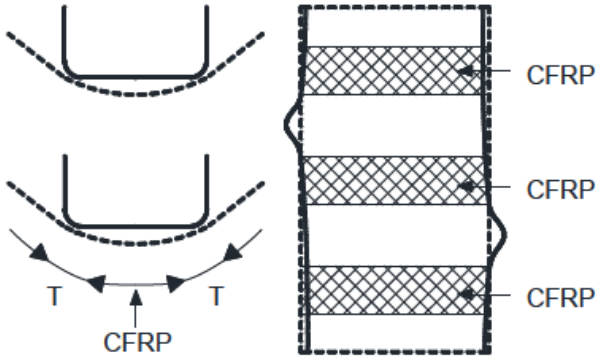

Figure 10: Buckling modes for long and short steel channels

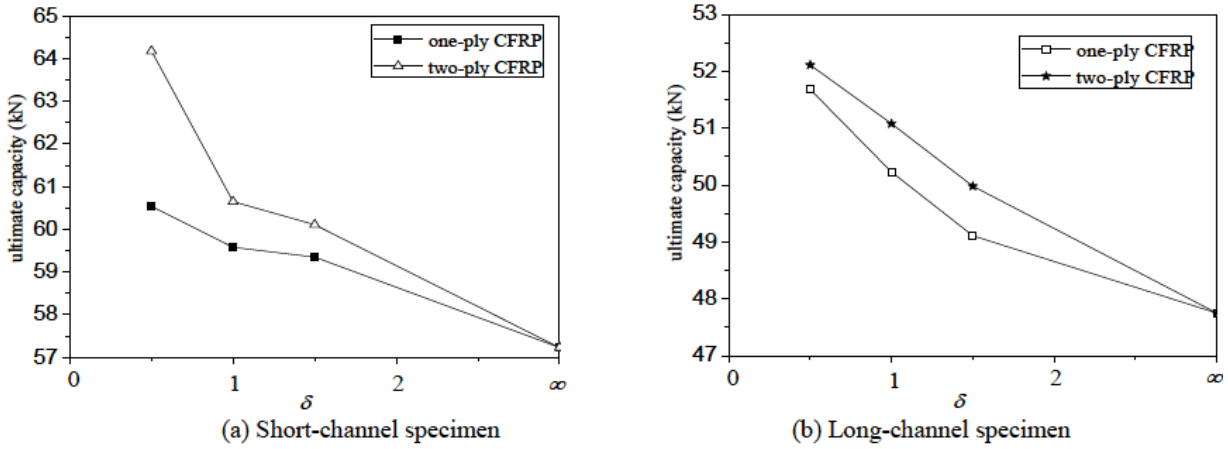

Figure 11: The relationship of buckling load capacity and ratio (δ)

4.2 Effect of CFRP layer and clear spacing of CFRP strips on ultimate capacity of short-channel specimens

The ultimate load capacity of CFRP-retrofitted specimens was improved in varying degrees. With two layers of CFRP specimens (SC2, SC4 and SC6), their capacity was greater than those with only one layer of CFRP (SC1, SC3 and SC5). When the clear spacing between the CFRP Strips is different, the ultimate load capacity is varied. This shows that although the increase of CFRP layer can improve the ultimate capacity, but the extent of the increase is also affected by the clear spacing. Similar conclusions can be obtained for the long-channel specimens.

In order to further study the effect of CFRP strips spacing on the ultimate load capacity of reinforced specimens, a parameter (δ) which is equal to the ratio of the clear spacing (s, Figure 1.) to the height of the web (h, Table 2) is determined by Eq. 7.

$$\delta = s/h_w \tag{7}$$

The relationship of the ultimate load capacity of the short-channel specimens and the ratio (δ) is shown in Figure 11*a*. When the clear spacing (s) is 50 mm, the ultimate capacity of specimens SC1 and SC2 were increased 5.8% and 12.1% respectively. This shows that when the ratio (δ) is equal to 0.5, the CFRP layer plays an important role in improving the ultimate capacity of the specimen.

With a clear spacing (s) of 100mm, the ultimate capacity of specimens SC3 and SC4 is increased 4.1% and 6%. The result shows that when the ratio (δ) is equal to 1, although the increase of CFRP layer can improve the ultimate capacity, there is no significant effect.

With a clear spacing (s) of 150mm, the ultimate capacity of specimens SC5 and SC6 is increased 3.7% and 5%. When the ratio (δ) is equal to 1.5, the CFRP strip is invalid because of the relative increment of SC5 and SC6.

4.3 Effect of CFRP layer and clear spacing of CFRP strips on ultimate capacity of long-channel specimens

The relationship of the ultimate load capacity of the long-channel specimens and the ratio (δ) is shown in Figure 11*b*. As for the long-channel specimens, when the clear spacing (s) was 50 mm, the ultimate load capacity of specimen LC2 and LC1 was increased 9.13% and 8.23% respectively. Although the improvement of the ultimate capacity of specimen LC2 was more than that of specimen LC1, but was only increased 0.9% relatively. It indicates that although increasing the CFRP layer can improve the ultimate load capacity when the ratio (δ) equals to 0.5, there is no significant effective.

With a clear spacing (s) of 100 mm, the ultimate load capacity of specimen LC3 and LC4 was increased 5.20% and 6.97% respectively, but was only increased 1.77% relatively. This was nearly two times of the improvement when the ratio (δ) equals to 0.5. It indicates that when the ratio (δ) equals to 1, the CFRP layer number plays an important role in improving the ultimate bearing capacity of specimen.

But for the clear spacing of 150 mm, the ultimate load capacity of specimen LC5 and LC6 only increased 2.85% and 4.67% respectively. Since the relatively increments of specimen LC5 and LC6 is marginally, it is verified that CFRP is ineffective when the parameter (δ) equals to 1.5.

5 Conclusions

This paper has presented a study on the potential of strengthening the cold-formed thin-walled channel by using externally bonded CFRP strips. A series of eccentric and axial compression tests of steel channels reinforced by high-strength CFRP was conducted to obtain the local buckling and overall buckling behavior and strength of the channels. The failure behavior was observed, and the effect of CFRP layer and the clear spacing on the ultimate capacity of all specimens was compared. The conclusions of this study are as follows.

1. The ultimate load capacity of the cold-formed thin-walled short- and long-channel specimens with transversely bonded CFRP strips was improved in some extent. When the CFRP strips spacing is 50 mm and the CFRP layer number is two, for the short-channel specimens under eccentrically load, the ultimate buckling load capacity can achieve an increase of 12.1%, but that of the long-channel specimens under axial load only be increased by 9.13%.
2. When the clear spacing of CFRP strips is greater than the web height of steel channel, that is δ>1, the transversely bonded CFRP does not have a significant improvement in buckling load capacity of the short- and long-channel components. While the clear spacing is less than the web height, that is $\delta \leq 1$, the more number of CFRP layer, the more enhancement of buckling load capacity.
3. The failure mode of the long-channel specimens were all the same as the overall flexural torsional buckling, and cannot be changed by transversely bonded CFRP strips. However, parts of failure modes of the short-channel specimens were changed from the flange local buckling to the overall flexural torsional buckling by transversely bonded CFRP strips, and the others remained the flange local buckling unchanged.
4. This paper only analyzes the buckling behavior of the cold-formed thin-walled short and long steel channels in the situation that transversely bonded CFRP strips under eccentric and axial load, respectively. As for the other orientation, such as longitudinally bonded CFRP or no spacing between the transverse CFRP strips, further work is needed to examine the behavior of the component under these conditions.

Acknowledgement: This study was generously funded by Xihua University key fund (z1120634) and the Ministry of education Chunhui project (Z2016156). The authors are most grateful to these organizations for their valuable support.

Conflict of Interests: The authors declare that there is no conflict of interests regarding the publication of this paper.

Notation

b	The flange width
E_f	Tangent elastic modulus of CFRP
f_{td}	Tensile strength of CFRP
h	Height of the web
L	Length of the specimen
r	radius of gyration about weak axis
s	The clear spacing of CFRP strips
t_f	Thickness of CFRP
t_w	Thickness of the web and flange

References

[1] AISC (2011). Steel construction manual, 14th ed., American Institute of Steel Construction.

[2] Cao, J. (2011). The Theoretical Analysis and Experimental Study of CFRP Reinforced Steel Structure, PhD Thesis. Hefei University of Technology, Hefei, China.

[3] Chen, T., Qi, M., Gu, X.L., Guo, D.M. (2013), "Experimental study on behavior of rectangular hollow steel section beams with initial crack retrofitted with CFRP plate", Journal of Building Structures, S1, pp. 71-76.(in Chinese)

[4] Edberg, W., Mertz, D., Gillespie, Jr J. (1996), "Rehabilitation of Steel Beams Using Composite Materials. Proceedings of the Materials Engineering Conference", Materials for the new Mllenium. New York, NY: ASCE, pp. 502-508.

[5] Elchalakani, M. and Fernando, D. (2012), "Plastic mechanism analysis of unstiffened steel I-section beams strengthened with CFRP under 3-point bending", Thin-Walled Structures, Vol. 53, pp. 58-71,

[6] Haedir, J. and Zhao, X. (2011),"Design of short CFRP-reinforced steel tubular columns", Journal of Constructional Steel Research, Vol. 67, No. 3, pp.497-509.

[7] Harries, K.A., Enhancing Stability of Steel Structural Sections using FRP Composites, Chapter 5 in Rehabilitation of Metallic Civil Infrastructure Using Fibre Reinforced Polymer Composites, V. Karbhari, editor. Woodhead Publishing Series in Civil and Structural Engineering No. 51, pp 117-139. ISBN-13: 978 0 85709 653 1

[8] Harries, K. A., Peck, A. and Abraham, E.J. (2009), "Enhancing stability of structural steel sections using CFRP", Thin–Walled Structures, Vol. 47, No. 10, pp. 117-139.

[9] Huo, J.Ha, Wang, L.G, Zhang, H.F, Liu, S.C. (2015), "Experimental research on prestressed CFRP sheets strengthened corroded

steel beams", Journal of Building Structures, Vol. 36, No. 11, pp. 72-78. (in Chinese)

[10] Liu, X., Silva, P. F., Mnni, A. (2001), "Rehabilitation of Steel Bridge Members with FRP Composite Materials" Proc.CCC2001, Composites in Construction, Porto, Portugal.

[11] Park, Jai-Woo *et al.* (2013), "Axial Loading Tests and FEM Analysis of Slender Square Hollow Section (SHS) Stub Columns Strengthened with Carbon Fiber Reinforced Polymers", International Journal of Steel Structures, Vol. 13, No. 4, pp. 731-743.

[12] Patnaik, A. K., Bauer, C. L. (2004). "Strengthening of Steel Beams with Carbon FRP Laminates", Advanced Composite Materials in Bridges and Structures. Calgary, Alberta.

[13] Peng, F.M., Hao, J.P., Yue, Q.R. (2005), "Elastic stability analysis of axially loaded compression steel members by FRP strengthening", Steel Structure, No. 3, pp. 17-20. (in Chinese)

[14] R. Sen and L. Liby. (1994), "Repair of steel composite bridge sections using CFRP laminates", US Department of Transportation Contract B-7932. University of South Florida. Tampa, Fla, USA,

[15] Sawulet, Bekey, Feng, P., Ye, L.P., *et al.* (2012), "Experimental study on CFRP fast anti-bucking strengthening technique for axial compressive steel members", Engineering Mechanics, No. 6, pp. 105-113. (in Chinese)

[16] Shulley, S. B., Huang, X., Karbhari, V. M., *et al.* (1994). "Fundamental Consideration of Design and Durability in Composite Rehabilitation Schemes for Steel Girders with Web Distress". Proceedings of the Third Materials Engineering Conference. San Diego, California.

[17] Standards China. Metallic materials: tensile testing: part 1: method of test at room temperature (GB/T 228.1-2010). Beijing, 2010. (in Chinese)

[18] Standards China. Technical code of cold-formed thin-wall steel structures (GB50018-2002). Beijing: 2002. (in Chinese)

[19] Sundarraja, M. C., Sriram, P., Ganesh Prabhu, G. (2014), "Strengthening of Hollow Square Sections under Compression Using CFRP Composites", Advances in Materials Science and Engineering, Article ID 396597.

[20] Tavakkolizadeh, M., Saadatmanesh, H. (2003), "Fatigue Strength of Steel Girders Strengthened with CFRP patch", Journal of Structural Engineering, Vol. 129, No. 2, pp. 186-196.

[21] Teng, J.G. and Hu, Y.M. (2007), "Behaviour of FRP-jacketed circular steel tubes and cylindrical shells under axial compression", Construction and Building Materials, No. 21, pp. 827–838.

[22] Miller, T.C., Chajes, M.J., Mertz, D.R., *et al.* (2001), "Strengthening of Steel Bridge Girder Using CFRP Plates", Journal of Bridge Engineering, Vol. 6, No. 6, pp. 514-522.

[23] Zhao, X.L., Zhang, L. (2007). "State-of-the-art-review on FRP strengthened steel structures", Engineering Structures, No. 29, pp. 1808–1823.